Materials Transactions, Vol. 49, No. 6 (2008) pp. 1486 to 1489

Improvement of Glass Forming Ability of Cu-Ni-Zr-Ti Alloys by Substitution of Hf and Nb

Dong-Myoung Lee[1,2]*, Ju-Hyun Sun[2], Seung-Yong Shin[2], Jeong-Chan Bae[2] and Chi-Hwan Lee[1]

[1]*Department of Metallurgical Engineering, Inha University, Nam-gu, Incheon, 402-751, Korea*
[2]*Advanced Functional Material Team, Korea Institute of Industrial Technology, Yeonsu-Gu, Incheon, 406-130, Korea*

New bulk metallic glasses exhibiting a high glass forming ability were formed by a substitution of Hf and Nb for Zr and Ti in quaternary Cu-Ni-Zr-Ti system. An 8 mm-diameter BMG rod was obtained at the $Cu_{50}Ni_8Zr_{15}Hf_3Ti_{23}Nb_1$ composition by suction casting method. The glass transition temperature, crystallization temperature and reduced glass transition temperature of the BMG were 699 K, 754 K, and 0.59, respectively. Making an alloy system more complex was useful to increase the GFA. [doi:10.2320/matertrans.MRP2008066]

(Received February 25, 2008; Accepted April 2, 2008; Published May 14, 2008)

Keywords: *metallic glass, glass forming ability, solidification, intermetallic alloys*

1. Introduction

The attractiveness of bulk metallic glasses (BMGs) has been recognized in recent years due to their unique properties that are rarely found in crystalline materials. Many recent investigations have focused on finding BMGs in multi-component alloy systems such as Pd-, Zr-, Ti-, and Cu-based system.[1–4] However, their potential applications have been very limited because of the high price of raw materials or a low glass forming ability (GFA). In order to extend the range of fields for BMG application, BMGs with high GFA need to be developed from easily available commercial materials.

Many Cu-based BMGs have been found in Cu-Zr,[5] Cu-Zr-Ti,[3] Cu-Ti-Zr-Ni,[6] Cu-Zr-Al,[7] Cu-Zr-Ti-(Y,Be),[8,9] and Cu-Zr-Ti-Ni-Si[10] alloy systems over the past decade. By adding elements in the Cu-Zr alloy system, the GFA of the Cu-based alloys was increased from 2 mm (binary) to 7 mm (quinary). It is well known that the Cu-Zr binary eutectics would present an easy glass former due to the low-lying eutectics over the central part of the phase diagram. Also the Ti-Ni, Zr-Ni, and Ti-Cu alloy systems have a potential to form metallic glasses according to A. Peker.[2] Therefore, it is assumed that an alloy system combined with Cu, Zr, Ni, and Ti element can exhibit an excellent GFA.

Of the Cu based BMGs mentioned above, the first three examples, Cu-Zr, Cu-Zr-Ti, Cu-Ni-Zr-Ti system,[5,7,8] have attracted our research attention. The GFA of Cu-based alloys were further enhanced by the partial replacement of Cu by Ni and of Zr by Ti. These BMGs development procedure shows one characteristic that Ni and Ti form a complete solid solution with Cu and Zr, respectively. It is thus considered that the additional element forming a complete solid solution with a major element is beneficial to form a metallic glass. Therefore in this study the $Cu_{54}Ni_6Zr_{22}Ti_{18}$ BMG whose GFA is 6 mm-diameter[11] was selected, and candidate elements capable of enhancing the GFA of the alloy were chosen according to the phase diagrams between the main and additional elements. Hf and Nb were selected since they form a complete solid solution with Zr and Ti, respectively.

Therefore, this paper aims to increase the GFA of the Cu-Ni-Zr-Ti alloys by adding the elements Hf and Nb. In addition, the thermal properties of the Cu-Ni-Zr-Ti quaternary alloys with respect to Hf and Nb substitution are investigated and the effect of the element addition is discussed.

2. Experimental Procedures

Pure metals Cu, Ni, Zr, Ti, Hf, and Nb, all at 99.99% purity, were weighed to give the required composition. Master alloys of 40Cu60Hf and 50Ni50Nb (mass%) were used to ensure a homogenous melting because the melting point of Hf (2506 K) and Nb (2750 K) are so high that the elements are hardly soluble into the melt. Mixtures of the elements were then alloyed and remelted four times in the arc melter. For rapid solidification of the alloys, they were cast by an arc suction casting method,[11] and to compare the BMG with ribbon metallic glass, which is considered to have a fully amorphous structure, the melt-spun ribbon exhibiting a thickness of about 30 μm and a width of about 3 mm was produced by the melt spinning method.[11] Structures of the amorphous specimens were identified by X-ray diffractometry (XRD, D8, Discover, Bruker) using a Cu-Kα source. The interior of rods were cut longitudinally in half and the cross-sectional surfaces were examined by the XRD to ensure the amorphicity of the interior of the rods. The glass transition and crystallization of the glassy alloys were examined by differential scanning calorimetry (DSC, Q100, TA Instruments) at a heating rate of 0.67 K/s in a copper pan. The melting temperatures of alloys were measured using differential thermal analysis (DTA, Q600, TA Instruments) at a heating rate of 0.167 K/s under a flowing 99.99% Ar atmosphere. The samples for DTA were placed in an alumina crucible whose inside was also covered with Y_2O_3 powders to prevent a reaction between the crucible and molten alloy. The microstructure of the sample was observed by scanning electron microscopy (SEM, JSM5510, JEOL), and the chemical composition of the phase was analyzed by electron probe micro-analyzer (EPMA, JXA-8900R, JEOL). Room temperature uniaxial compressive tests were conducted on the cylindrical cast rods with a diameter of 2 mm and a height

*Graduate Student, Inha University

of 4 mm using the Instron-type test machine under the constant strain rate of $5 \times 10^{-4}\,s^{-1}$. Microstructure of the tested specimen was observed the SEM.

3. Results

The pseudo-ternary composition region showing bulk glass formation over 6 mm-diameter that is superior to the GFA of $Cu_{54}Ni_6Zr_{22}Ti_{18}$ alloy is illustrated in Fig. 1(a). The diagram is expressed as pseudo-ternary because Cu, Zr and Ti were interchangeable with Ni, Hf and Nb, respectively. The data on Cu/Ni, Zr/Hf and Ti/Nb ratios are not presented. More detailed descriptions of the BMGs can be found in Ref. 12). In the composition region, the best glass former was $Cu_{50}Ni_8Zr_{15}Hf_3Ti_{23}Nb_1$ composition whose GFA was 8 mm-diameter confirmed by the suction casting method. The structure in the center of the rod was identified by the XRD to be that shown in Fig. 1(b). No peaks corresponding to crystalline phases were observed in the 8 mm-diameter sample while the 9 mm-diameter sample showed sharp diffraction peaks superimposed on a weak halo pattern.

Figure 2(a) and (b) shows the DSC curves obtained from the ribbon and bulk amorphous $Cu_{50}Ni_8Zr_{15}Hf_3Ti_{23}Nb_1$ alloy. The glass transition temperature (T_g) and onset temperature of first crystallization (T_x) of the amorphous

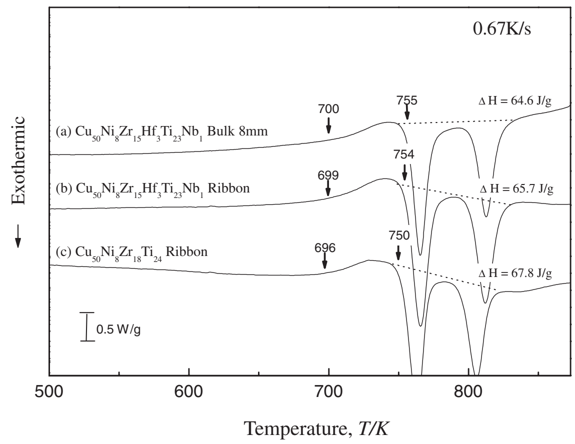

Fig. 2 DSC traces obtained from the ribbon and bulk amorphous alloys.

alloys were nearly the same for both the ribbon and bulk samples. The integrated heat of the exotherms (ΔH) of the bulk specimen was also the same as that of the ribbon specimen, indicating that a fully amorphous structure was obtained in the bulk rod. The melt-spun alloy showed T_g of 699 K and T_x of 754 K. The supercooled liquid range ($\Delta T_x = T_x - T_g$) was about 55 K.

In order to examine the adding effect of Hf and Nb on the GFA, Hf and Nb element in the $Cu_{50}Ni_8Zr_{15}Hf_3Ti_{23}Nb_1$ alloy included to Zr and Ti elements in the alloy, respectively, and the $Cu_{50}Ni_8Zr_{18}Ti_{24}$ alloy was prepared and compared with the $Cu_{50}Ni_8Zr_{15}Hf_3Ti_{23}Nb_1$ alloy. Thermal properties of these alloys are given in Figs. 2 and 3. The T_g and T_x of the $Cu_{50}Ni_8Zr_{18}Ti_{24}$ alloy without Hf and Nb were slightly lower than the $Cu_{50}Ni_8Zr_{15}Hf_3Ti_{23}Nb_1$ alloy as shown in Figs. 2(a) and (c), but the GFA of both alloys was different: 8 mm-diameter for $Cu_{50}Ni_8Zr_{15}Hf_3Ti_{23}Nb_1$ and 6 mm-diameter for $Cu_{50}Ni_8Zr_{18}Ti_{24}$ alloy. Figure 3 shows DTA traces obtained from the crystalline alloys. Their solidus temperatures (T_s) that are assumed eutectic temperature are all around 1104 K. However, the liquidus temperatures (T_l) of the alloys are different. The T_l of the $Cu_{50}Ni_8Zr_{15}Hf_3Ti_{23}Nb_1$ is only 2∼3 K higher than that of the $Cu_{50}Ni_8Zr_{18}Ti_{24}$ alloy. From the results of Figs. 2 and 3, the reduced glass transition temperature ($T_{rg} = T_g/T_l$) of the

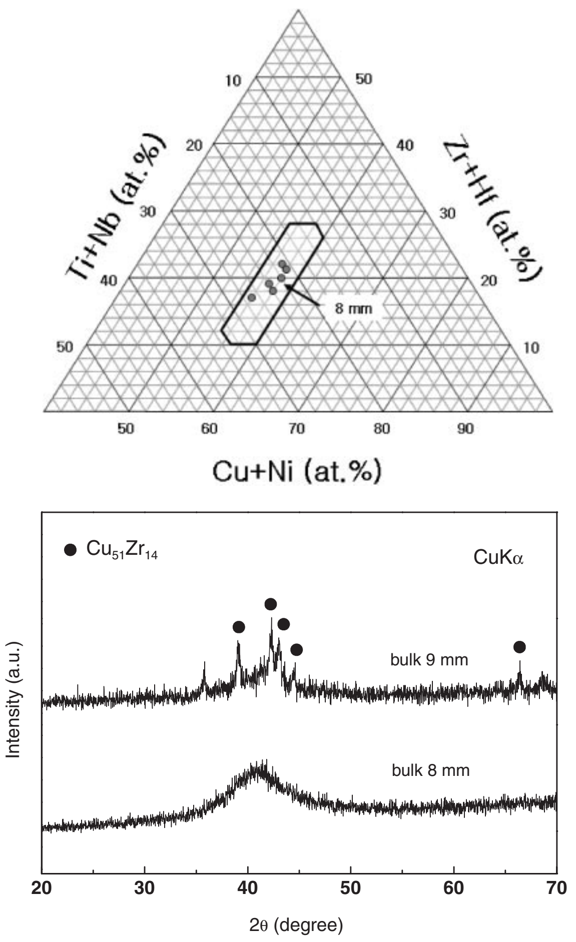

Fig. 1 (a) Pseudo-ternary phase diagram showing compositional range of the bulk amorphous alloys. (b) XRD patterns obtained from the suction cast $Cu_{50}Ni_8Zr_{15}Hf_3Ti_{23}Nb_1$ alloy.

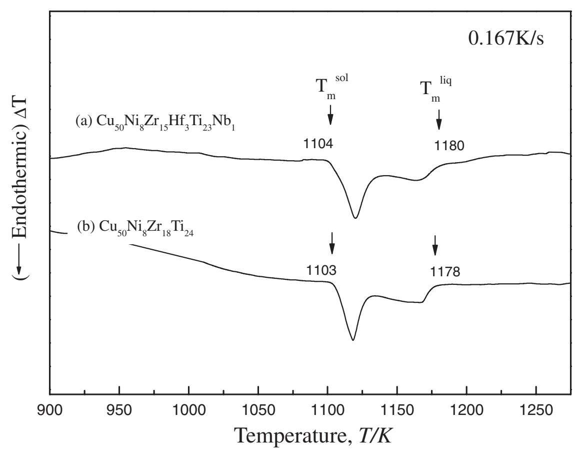

Fig. 3 DTA traces obtained from the equilibrium crystalline alloys.

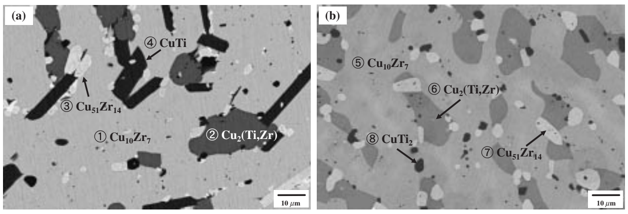

Alloy	Phase label	Composition (at %)						Phase
		Cu	Ni	Zr	Hf	Ti	Nb	
(a) $Cu_{50}Ni_8Zr_{18}Ti_{24}$	①	48.4	9.4	22.1	-	20.1	-	$Cu_{10}Zr_7$
	②	37.3	11.9	8.2	-	42.8	-	Cu_2(Ti,Zr)
	③	74.8	1.4	21.1	-	2.7	-	$Cu_{51}Zr_{14}$
	④	47.5	1.9	1.5	-	49.1	-	CuTi
(b) $Cu_{50}Ni_8Zr_{15}Hf_3Ti_{23}Nb_1$	⑤	46.3	10.9	22.2	0.2	20.4	-	$Cu_{10}Zr_7$
	⑥	41.4	7.4	15.5	0.2	31.2	4.3	Cu_2(Ti,Zr)
	⑦	75.6	1.7	20.5	-	2.2	-	$Cu_{51}Zr_{14}$
	⑧	20.8	12.6	6.3	0.4	58.5	1.4	$CuTi_2$

Fig. 4 Back scattered electron images of the (a) $Cu_{50}Ni_8Zr_{18}Ti_{24}$ and (b) $Cu_{50}Ni_8Zr_{15}Hf_3Ti_{23}Nb_1$ alloys, and their corresponding phase compositions measured from the EPMA (The alloys were heat-treated at 1083 K for 24 h and furnace-cooled to room temperature at a rate of 1 K/min).

two alloys was calculated to be same 0.59 despite their different GFA.

Microstructures of the $Cu_{50}Ni_8Zr_{18}Ti_{24}$ and $Cu_{50}Ni_8Zr_{15}Hf_3Ti_{23}Nb_1$ alloys are shown in Fig. 4. The alloys were heat-treated at 1083 K (near their solidus temperature) for 24 h and furnace-cooled to room temperature at a rate of 1 K/min to examine the phases near equilibrium state at room temperature, and the compositions of their constituent phases were analyzed by the EPMA. Based on the EPMA result, it is assumed that the $Cu_{10}Zr_7$, Cu_2(Zr,Ti), and $Cu_{51}Zr_{14}$ phases were crystallized in the both alloys, but the different phases of CuTi and $CuTi_2$ were observed in the $Cu_{50}Ni_8Zr_{18}Ti_{24}$ and $Cu_{50}Ni_8Zr_{15}Hf_3Ti_{23}Nb_1$ alloys, respectively, which implies the change in the crystallization behavior by the substitution of Hf and Nb. In addition, it is observed that the additives of Hf and Nb are dissolved in the Cu_2(Zr,Ti) and $CuTi_2$ phases of the $Cu_{50}Ni_8Zr_{15}Hf_3Ti_{23}Nb_1$ alloy.

Figure 5(a) shows the compressive stress-strain curve of the bulk amorphous $Cu_{50}Ni_8Zr_{15}Hf_3Ti_{23}Nb_1$ rod with 2 mm-diameter. The curve shows linear elastic behavior up to yielding, followed by plastic strain of about 1.2%. The compressive fracture strength and fracture strain are approximately 2140 MPa and 3.0%, respectively. The SEM images of the fractured specimen show vein patterns, a typical fracture characteristic of amorphous alloys and compressive fracture took place along maximum shear plane declined 45° to the loading direction as shown in Fig. 5(b) and (c).

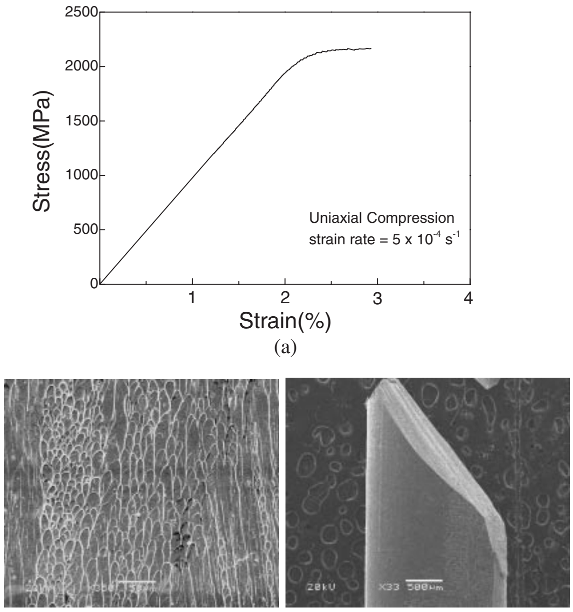

(b) (c)

Fig. 5 Compressive stress-strain curve (a) and fracture surfaces (b), (c) of the bulk amorphous $Cu_{50}Ni_8Zr_{15}Hf_3Ti_{23}Nb_1$ alloy.

4. Discussion

Many Cu-based BMGs showing an increased GFA have been found. Among these BMGs, we focused on the four alloys presented in Table 1, which shows that a higher GFA was obtained with increasing complexity of the alloy systems. Interestingly, both the substituting and substituted elements of the alloy systems exhibited a complete solid solution. Therefore, we replaced Zr with Hf and Ti with Nb to obtain a higher GFA of the Cu-based BMG. As a result, a glassy rod with a maximum sample diameter of 8 mm was obtained from the composition of $Cu_{50}Ni_8Zr_{15}Hf_3Ti_{23}Nb_1$.

In order to explain the enhanced GFA of this alloy, we took into account both kinetic and thermodynamic factors. According to the "confusion principle",[13] with increasing number of components in the liquid alloy, crystallization becomes confused or frustrated. Specifically, the crystallization process of the multi-component, undercooled liquid will tend to become more sluggish than that of simpler systems. For the $Cu_{50}Ni_8Zr_{15}Hf_3Ti_{23}Nb_1$ alloy, the extraordinarily high GFA can be explained by the confusion principle. Furthermore, the Cu-Ni-Zr-Ti alloy system agrees well with the three empirical rules.[14] For instance, the heat of mixing between Cu-Zr is −23 kJ/mol, Cu-Ti is −17 kJ/mol, Ni-Zr is

Table 1 Thermal properties and GFA of the reported Cu-Zrbased alloys. (The melting temperature and GFA of the reference alloys were reexamined by the method used in this study. The values showed different from the values reported in the references)

Composition	T_g (K)	T_x (K)	ΔT_x (K)	T_s (K)	T_l (K)	T_{rg} (T_g/T_l)	GFA (mm)	Ref.
$Cu_{64}Zr_{36}$	787	833	46	1158	1229	0.64	1	5)
$Cu_{60}Zr_{30}Ti_{10}$	713	750	37	1103	1247	0.57	5	4)
$Cu_{47}Ni_8Zr_{11}Ti_{34}$	671	717	46	1105	1162	0.58	6	6)
$Cu_{54}Ni_6Zr_{22}Ti_{18}$	712	769	57	1104	1186	0.60	6	11)
$Cu_{50}Ni_8Zr_{18}Ti_{24}$	696	750	54	1104	1178	0.59	6	Figs. 2, 3 (this study)
$Cu_{50}Ni_8Zr_{15}Hf_3Ti_{23}Nb_1$	699	754	55	1104	1180	0.59	8	Figs. 2, 3 (this study)

−49 kJ/mol and Ni-Ti is −35 kJ/mol.[15] In addition, the atom radii of the component atoms are 0.127 nm for Cu, 0.124 nm for Ni 0.155 nm for Zr, 0.155 for Hf, 0.140 nm for Ti, and, 0.145 nm for Nb.[16] The Hf and Nb additives have negative heats of mixing between Hf-Cu (−17 kJ/mol), Hf-Ni (−42 kJ/mol) and Nb-Ni (−30 kJ/mol).

As shown in Fig. 4, the crystallization behavior by the substitution of Hf and Nb in the $Cu_{50}Ni_8Zr_{18}Ti_{24}$ alloys was changed, and the Hf and Nb are dissolved in the Cu_2(Zr,Ti) and $CuTi_2$ phases of the $Cu_{50}Ni_8Zr_{15}Hf_3Ti_{23}Nb_1$ alloy. Moreover, since the Cu_2(Zr,Ti) and $CuTi_2$ phases are intermetallics that need long range diffusion of atoms for their crystallization, the crystallization from the liquid phase can be more frustrated. Therefore, the partial substitution of Zr with Hf and of Ti with Nb did not increase its melting point greatly but restrict the kinetic diffusion of atoms due to the multi-component alloy system.

In general, T_{rg} is used as a parameter that determines the GFA of an alloy.[17] We considered this parameter to explain the enhanced GFA achieved by the addition of elements. Table 1 shows the thermal properties and the corresponding T_{rg} of the Cu-based BMGs. In case of the Cu-Zr based alloy systems, their GFA is inversely proportional to their T_{rg}, but the GFA is proportional to the complexity of the alloy system. The parameter T_{rg} does not sufficiently account for the enhanced GFA, which is similar to the BMGs reported in the Ref. 18, 19). Specifically, the multi component alloys except for the Cu-Zr alloy seem to have one solidus temperature around 1104 K which is lower than that of the Cu-Zr alloy. It is thus assumed that the multi component alloys share the one eutectic point, i.e. they are all scattered from the eutectic composition. From a kinetic view, around eutectics in Cu-Ni-Zr-Ti systems, there are multiple ordered intermetallic phases competing with each other, and the crystallization of the liquid requires simultaneous rearrangement of different species of atoms, which significantly limits the kinetics of the process and thus promote glass formation. If the Hf and Nb are solved into the intermetallic phases for Zr and Ti involved in the eutectic reaction, the crystallization of the liquid is more restricted and GFA of the liquid can be enhanced. Therefore, it is thought that making alloy complex by substitution of complete solid solution element can be a useful way for improving GFA of an alloy.

5. Conclusion

A Cu-based BMG having high GFA and large ΔT_x were developed in a Cu-Ni-Zr(Hf)-Ti(Nb) alloy system by substitution of Hf and Nb for Zr and Ti, respectively. At the $Cu_{50}Ni_8Zr_{15}Hf_3Ti_{23}Nb_1$ alloy composition, a fully amorphous, 8 mm-diameter rod was formed by copper mold suction casting. The T_g, T_x, ΔT_x and T_l of this BMG were 699, 754, 55 and 1180 K, respectively. We therefore concluded that the Hf and Nb substitution in quaternary Cu-Ni-Zr-Ti systems was effective in enhancing the GFA due to increase in the complexity of the system.

REFERENCES

1) A. Inoue, N. Nishiyama and H. Kimura: Mater. Trans., JIM **38** (1997) 179–183.
2) A. Peker: Ph.D. thesis, California Institute of Technology, 1993.
3) Y. C. Kim, W. T. Kim and D. H. Kim: Mater. Trans., JIM **43** (2002) 1243–1247.
4) A. Inoue, W. Zhang, T. Zhang and K. Kurosaka: Acta Mater. **49** (2001) 2645–2652.
5) D. Xu, B. Lohwongwatana, G. Duan, W. L. Johnson and C. Garland: Acta Mater. **52** (2004) 2621.
6) X. H. Lin and W. L. Johnson: J. Appl. Phys. **79** (1995) 6514–6519.
7) A. Inoue and W. Zhang: Mater. Trans., JIM **43** (2002) 2921–2925.
8) T. Zhang, K. Kurosaka and A. Inoue: Mater. Trans., JIM **42** (2001) 2042–2045.
9) A. Inoue, T. Zhang, K. Kurosaka and W. Zhang: Mater. Trans., JIM **42** (2001) 1800–1804.
10) H. Choi-Yim, R. Busch and W. L. Johnson: J. Appl. Phys. **83** (1998) 7993–7997.
11) S. Y. Shin, J. H. Kim, D. M. Lee, J. K. Lee, H. J. Kim, H. G. Jeong and J. C. Bae: Mater. Sci. Forum **449–452** (2004) 945–948.
12) S. Y. Shin, J. C. Bae, J. H. Kim, D. M. Lee, K. I. Heo, J. H. Sun, H. J. Kim, J. K. Lee, T. S. Kim and H. G. Jeong: KR Patent 10-2005-0077859, August 24, 2005.
13) A. L. Greer: Nature **366** (1993) 303–304.
14) A. Inoue: Acta mater. **48** (2000) 279–306.
15) A. F. Wells: *Structural Inorganic Chemistry*, (Oxford University Press, Oxford, 1984) p. 1382.
16) F. R. Boer, R. Boom, W. C. M. Mattens, A. R. Miedema and A. K. Niessen: *Cohesion in Metals*, (North-Holland, Amsterdam, 1989) p. 1–758.
17) D. Turnbull: Contemp. Phys. **10** (1969) 473–488.
18) D. Xu., G. Duan and W. L. Johnson: Phys. Rev. Lett. **92** (2004) 245504-1-4.
19) Q. Zhang, W. Zhang, G. Xie and A. Inoue: Mater. Trans., JIM **48** (2007) 1626–1630.